GRADUATE AERONAUTICAL LABORATORIES
CALIFORNIA INSTITUTE OF TECHNOLOGY

FUNDAMENTAL STUDIES RELATING TO THE MECHANICAL BEHAVIOR OF SOLID PROPELLANTS, ROCKET GRAINS AND ROCKET MOTORS

P. J. Blatz
W. L. Ko
A. R. Zak

GALCIT SM 62-14 February 1962

Firestone Flight Sciences Laboratory

Guggenheim Aeronautical Laboratory

Karman Laboratory of Fluid Mechanics and Jet Propulsion

Pasadena

GALCIT 118 A - PROGRESS REPORT NO. 3

Aerojet Contract S-420061-OP

November 28, 1961 - February 28, 1962

FUNDAMENTAL STUDIES RELATING TO THE MECHANICAL BEHAVIOR OF SOLID PROPELLANTS, ROCKET GRAINS AND ROCKET MOTORS

P. J. Blatz
W. L. Ko
A. R. Zak

GALCIT SM 62-14 February 1962

This program is being supported by the Aerojet-General Corporation, Sacramento Division, under technical cognizance of Dr. F. J. Climent to provide technical support to the Polaris Project

Firestone Flight Sciences Laboratory
California Institute of Technology
Pasadena, California

TABLE OF CONTENTS*

* The contents of this quarterly progress report comprise only Chapters I and IV. Material for the other chapters will be included in subsequent reports also to be organized as indicated.

I. MECHANICAL BEHAVIOR OF RUBBERY MATERIALS

A. Introduction

The former reports provided considerable information about foam and continuum rubbers under three types of tensile loading (i.e. uniaxial, strip-biaxial and homogeneous-biaxial tension).

Since continuum rubbers are almost incompressible it is extremely difficult to determine the strain energy function beyond the linear term. On the other hand the highly dilatable foam rubber enables one to determine the functional form of the strain energy valid up to higher order terms. Special attention is being paid to foam rubber, since it represents the limiting case of completely dewetted propellant.

The present report will (i) furnish the method of determination of strain energy function and the associated constitutive stress-strain law for large deformations out to fracture and (ii) present the tri-axial tensile test data needed to double check item (i).

B. Determination of Functional Form of W and the Constitutive Law

For uniaxial tension:

From equation (I. 1), page 4, Progress Report No. 2

$$W_3 = -\mu\left[\frac{f}{\lambda} - \frac{(1-f)\lambda}{J_3^2}\right] \quad , \qquad J_3 = \lambda\lambda_{lat}^2 \tag{I. 1}$$

If we define Poisson's ratio ν in the following way,

$$J_3 = \lambda^{1-2\nu} \tag{I. 2}$$

The Poisson's ratio defined this way checks with the experimental data to high accuracy (c.f. Figure I. 1).

Using (I. 2), (I. 1) becomes,

$$\overline{W_3} = -\mu \left[f\, J_3^{-\frac{1}{1-2\nu}} - (1-f)\, J_3^{\frac{4\nu-1}{1-2\nu}} \right] \qquad \text{(I. 3)}$$

Integration yields,

$$\overline{W}(J_1, J_2, J_3) = \frac{\mu}{2} f \left[(J_1 - 3) + \frac{1-2\nu}{\nu} J_3^{-\frac{2\nu}{1-2\nu}} \right] + \frac{\mu(1-f)}{2} \left[(J_2 - 3) + \frac{1-2\nu}{\nu} J_3^{\frac{2\nu}{1-2\nu}} \right] \qquad \text{(I. 4)}$$

and the associative constitutive law (equation (I. 23) Progress Report No. 1) becomes,

$$\overline{\sigma_i} J_3 = \sigma_i \lambda_i = \mu f \left[\lambda_i^2 - J_3^{-\frac{2\nu}{1-2\nu}} \right] - \mu(1-f) \left[\frac{1}{\lambda_i^2} - J_3^{\frac{2\nu}{1-2\nu}} \right] \qquad \text{(I. 5)}$$

(i not summed)

Equations (I. 4), (I. 5) are the isothermal-equilibrium equations of state and are valid up to high strain.

For strip-biaxial tension:
From equation (I. 2), page 4, Progress Report No. 2

$$\overline{W_3} = -\mu \left[f \frac{J_3}{\lambda^2} - \frac{(1-f)\lambda^2}{J_3^3} \right] , \qquad J_3 = \lambda \lambda_{th} \qquad \text{(I. 6)}$$

Equating terms in (I. 3) and (I. 6), Poisson's ratio in strip-biaxial tension will be defined as

$$J_3 = \frac{1-2\nu}{1-\nu} \tag{I.7}$$

For Homogeneous-Biaxial Tension:
From equation (I. 3), page 4, Progress Report No. 2

$$W_3 = -\mu\left[\frac{f J_3}{\lambda^4} - \frac{(1-f)\lambda^4}{J_3^3}\right], \qquad J_3 = \lambda^2\lambda_{th} \tag{I.8}$$

Equating (I. 3) and (I. 8), Poisson's ratio in homogeneous-biaxial tension will be defined as

$$J_3 = \frac{2(1-2\nu)}{1-\nu} \tag{I.9}$$

The plots $\ln J_3$ vs $\ln\lambda$ for the above three types of test agree very well with the theoretical curves from equations (I. 2), (I. 7), and (I. 9), and the Poisson's ratio in the three tests gives $\nu = 1/4$, (c. f. Figure I. 1, I. 2, I. 3). Thus (I. 4) and (I. 5) must be universal functional expressions independent of the stress field. We shall see how this applies to the case of triaxial tension.

C. Summary of Previous data on PU-foam

Type of Test	Shear Modulus,	f	Poisson's Ratio,
Simple Tension	38 (psi)	0. 13	0. 25
Strip-Biaxial Tension	29	0. 07	0. 25
Homogeneous-Biaxial Tension	27	-0. 19	0. 25
Average Value	32	0	0. 25

D. Triaxial Tension

$$\lambda_i = \lambda , \qquad \lambda_j = \lambda_k = 1 \quad , \qquad J_3 = \lambda \tag{I. 10}$$

The constitutive law becomes,

$$\frac{\sigma_{tri}}{\mu} = \left[J_3^{\frac{2(1-\nu)}{1-2\nu}} - 1 \right] \left[f J_3^{-\frac{1}{1-2\nu}} + \frac{(1-f)}{J_3^3} \right] \tag{I. 11}$$

Since there are two parameters f and ν to be determined, one must be assumed and the other determined. With the information from the previous test data, we find that $\mu_{ave.} \approx 32$ psi , $f = 0$ and $\nu \approx 1/4$, and these can be checked with the test data in the following two ways:

i) If $f \approx 0$, (I. 11) yields

$$\left[\frac{\sigma_{tri}}{\mu} J_3^3 + 1 \right] = J_3^{\frac{2(1-\nu)}{1-2\nu}} \tag{I. 12}$$

ii) If $\nu \approx 1/4$; (I. 11) becomes,

$$\frac{\sigma_{tri}}{\mu \left(J_3 - 1/J_3^2 \right)} = f + (1-f) \frac{1}{J_3} \tag{I. 13}$$

For this test a thin circular disk of specimen (diameter ≈ 2 1/2" , thickness ≈ 1/4") was bonded both sides on metal (or plexiglass) flange (Figure I. 4) and the isothermal-equilibrium stresses were read from

the INSTRON. From the data the following curves were plotted (c.f. Figures I.5 to I.7).

i) σ_{tri} vs λ

ii) $\log_{10}\left(\frac{\sigma_{tri}}{\mu_{ave.}} J_3^{\,3} + 1\right)$ vs $\log_{10} J_3$

iii) $\frac{\sigma_{tri}}{\mu_{ave}\left(J_3 - \frac{1}{J_3^{\,2}}\right)}$ vs $\frac{1}{J_3}$

in the plots of (ii) and (iii) the average shear modulus $\mu_{ave} = 32$ psi was used (i.e. $\mu_{ave} = 1/3(\mu_{uni} + \mu_{st\text{-}bi} + \mu_{ho\text{-}bi}) = 32$ psi.

E. Results and Discussion

The strain energy function and the associated constitutive stress-strain law, universally good for uniaxial, strip-biaxial and homogeneous-biaxial stress fields, have been determined. The triaxial test points are so scattered that the stress-extension curve can hardly be drawn. This scattering is due to the early local tearing of the bonding surface. In the first three tests the specimens were bonded on the metal surfaces, while in the fourth one, it was bonded to a plexi-glass surface and evinced better adhesion. Figures I.6, I.7 reveal that the theoretical curves are a fairly good representation of the test data points. We shall continue this test by improving the bonding such that the early tearing may be eliminated.

FIG. I.1. DEPENDENCE OF UNIAXIAL DILATATION ON LONGITUDINAL EXTENSION RATIO

PU-FOAM

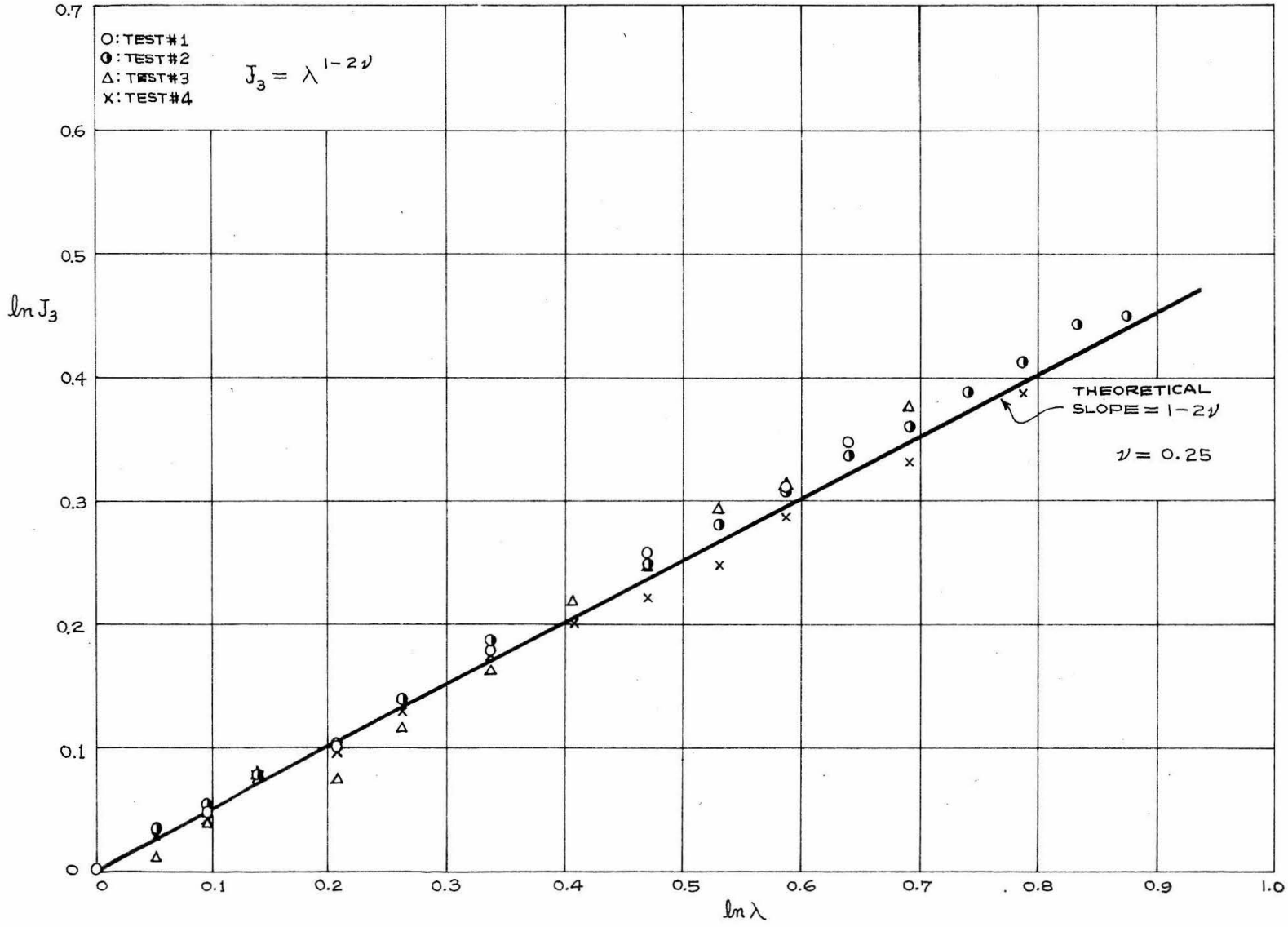

FIG. I.2. DEPENDENCE OF STRIP-BIAXIAL DILATATION ON LONGITUDINAL EXTENSION RATIO

PU-FOAM

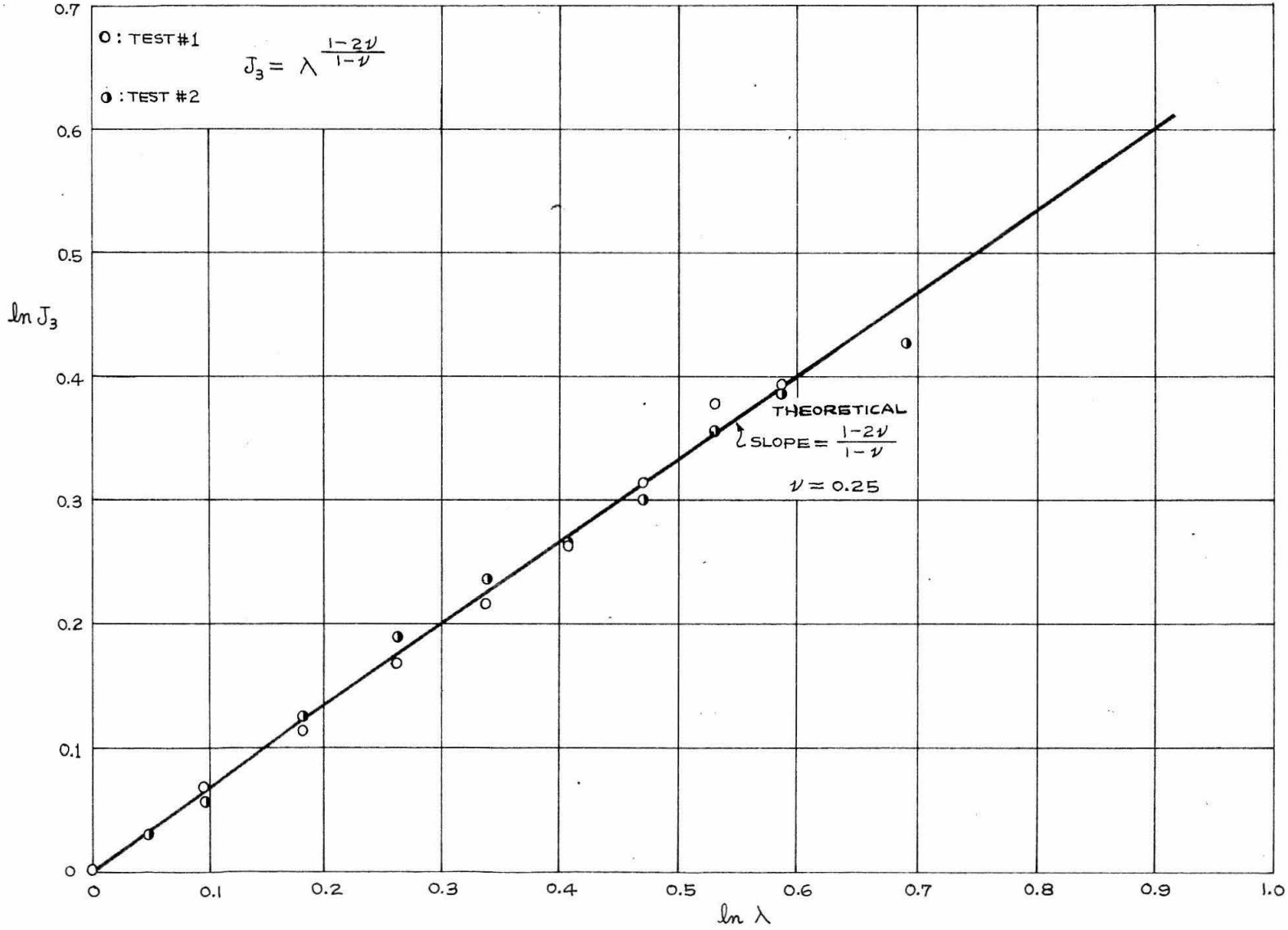

FIG. I. 3. DEPENDENCE OF HOMOGENEOUS-BIAXIAL DILATATION ON LONGITUDINAL EXTENSION RATIO

PU-FOAM

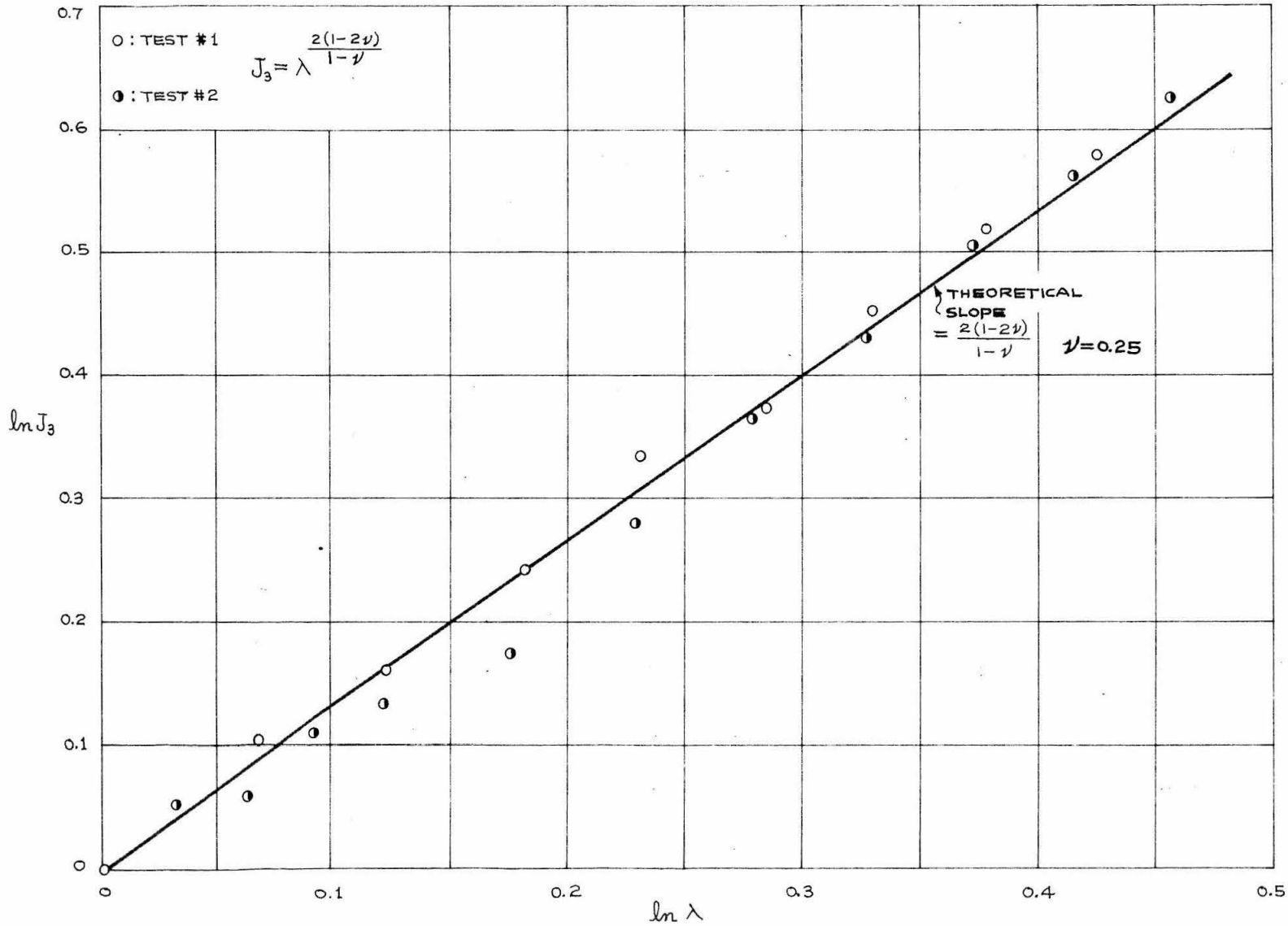

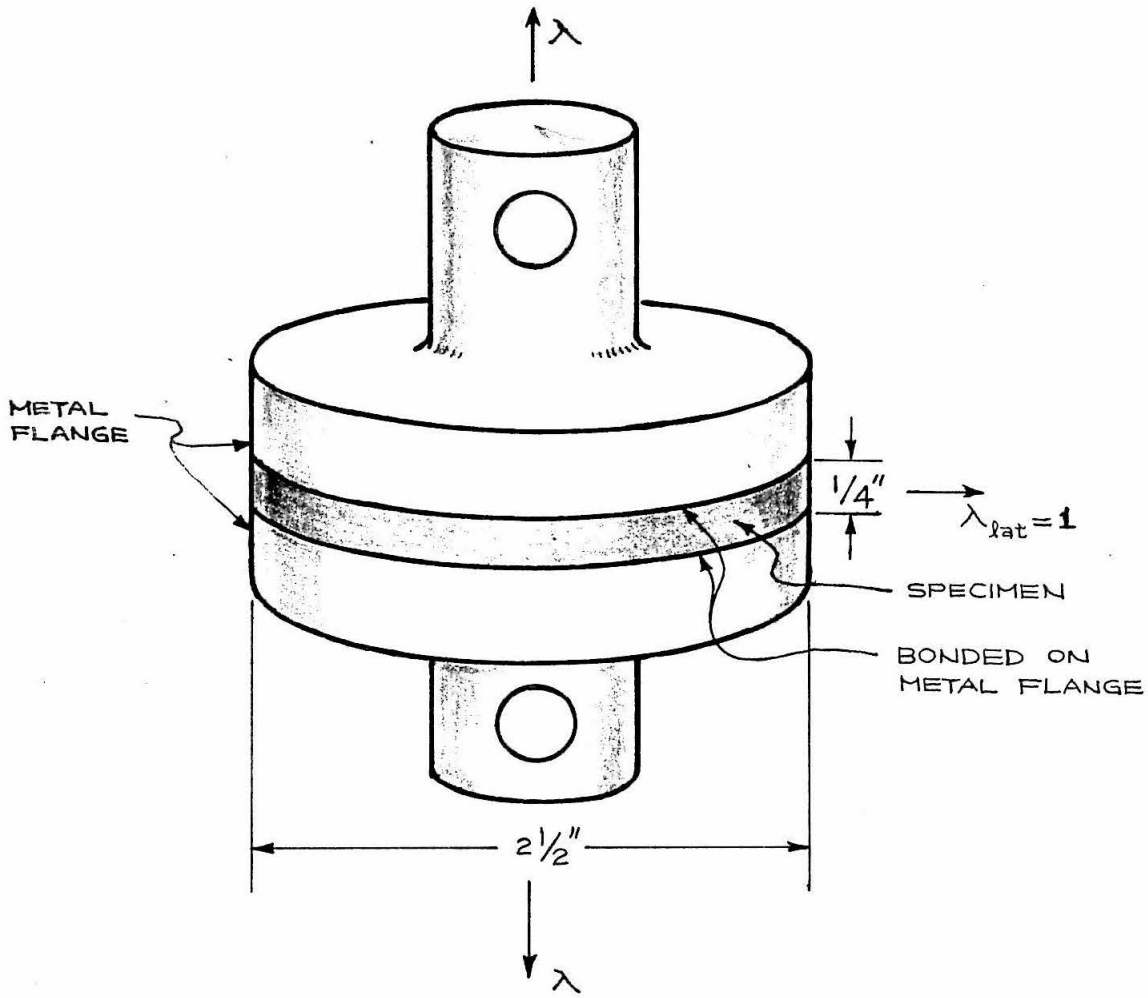

FIG. I.4. TRIAXIAL TENSION

FIG. I. 5. TRIAXIAL STRESS VS. LONGITUDINAL EXTENTION RATIO

PU-FOAM

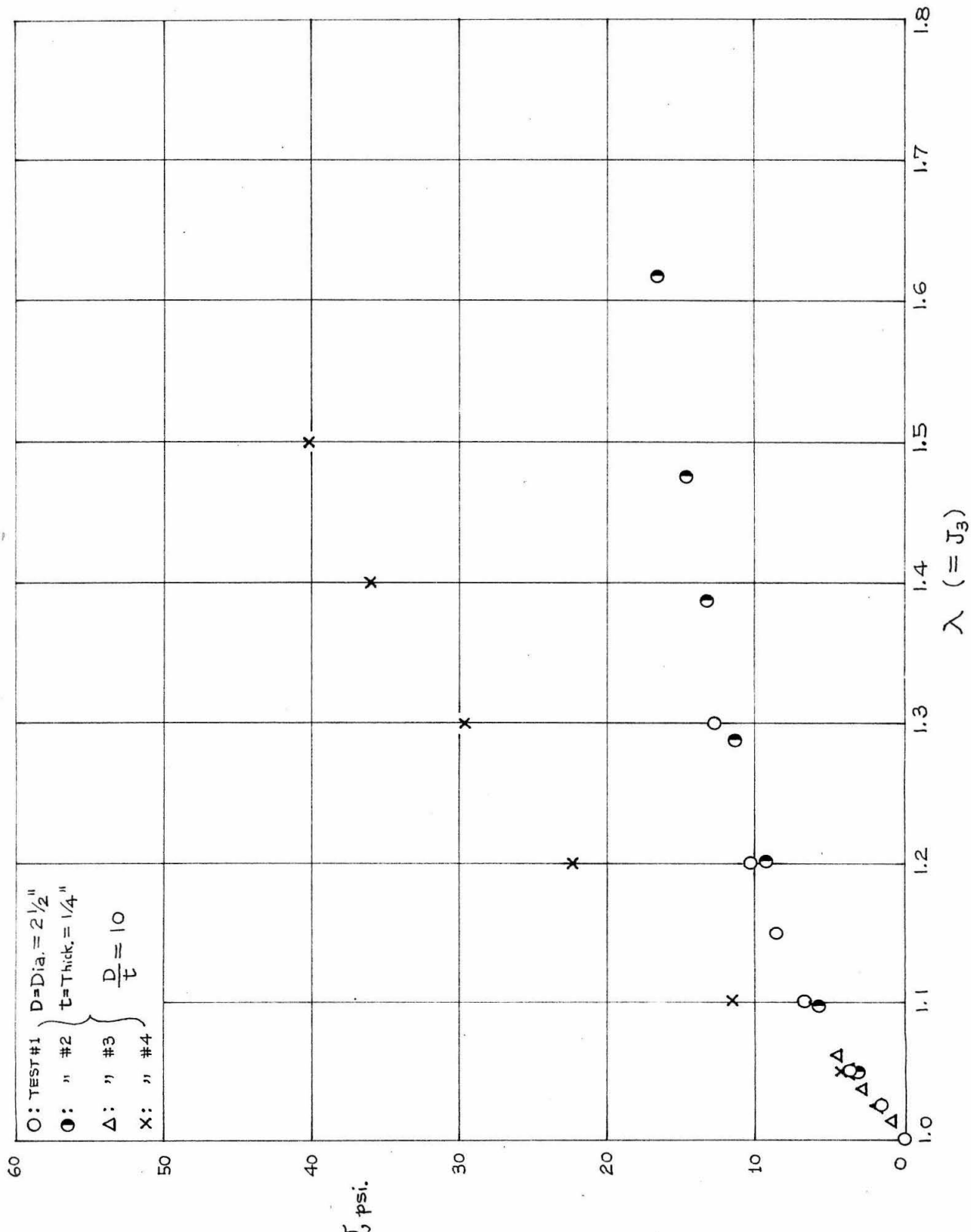

FIG. I. 6. EVALUATION OF ν FROM TRIAXIAL DATA. ASSUMPTION: $f=0$, $\mu=\frac{1}{3}(\mu_{uni}+\mu_{s\text{-}bi}+\mu_{tt\text{-}bi})=32$ psi.

PU-FOAM

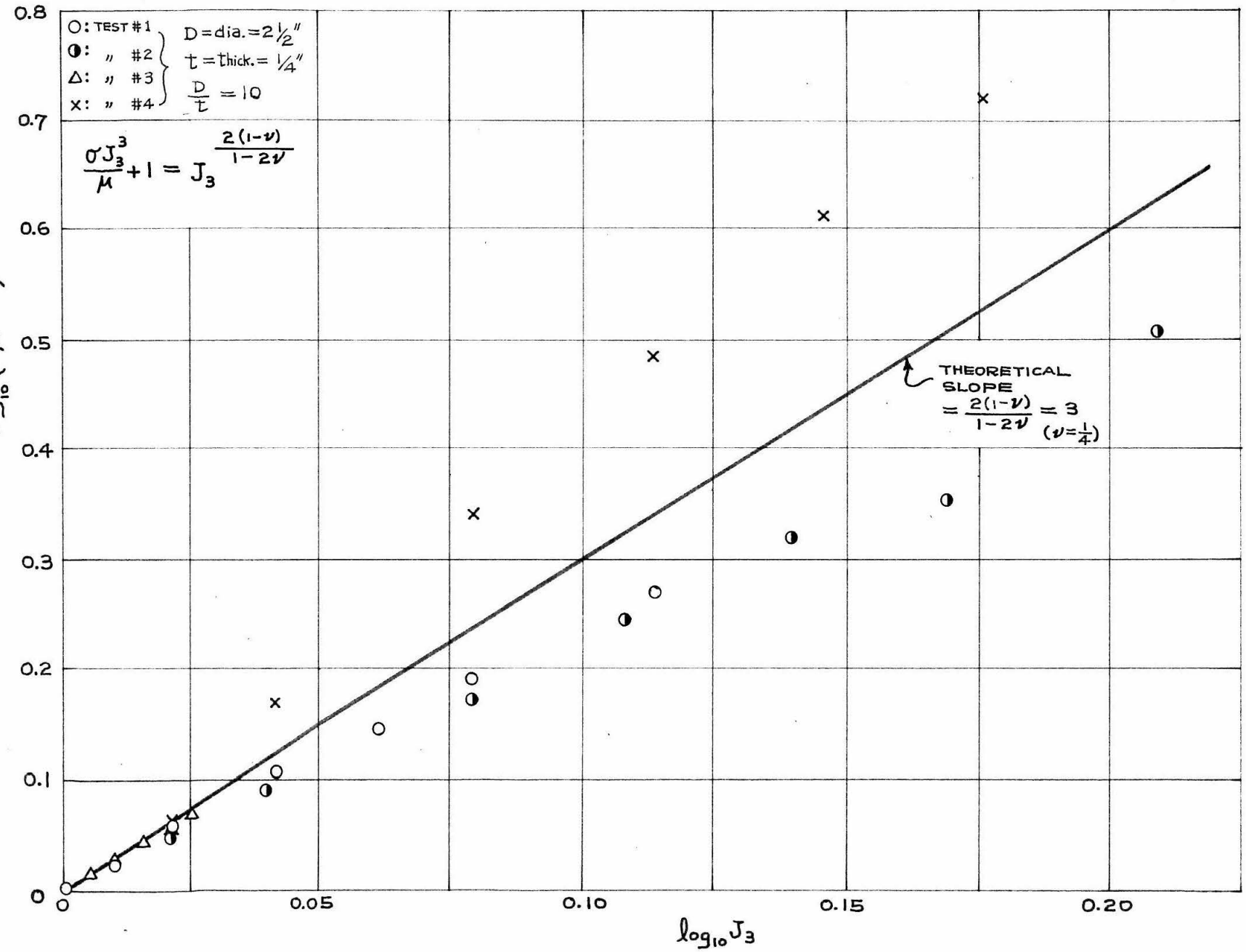

FIG. I.7. EVALUATION OF f FROM TRIAXIAL DATA. ASSUMPTION: $\nu = 1/4$, $\mu = \frac{1}{3}(\mu_{uni} + \mu_{s\text{-}bi} + \mu_{h\text{-}bi}) = 32$ psi.

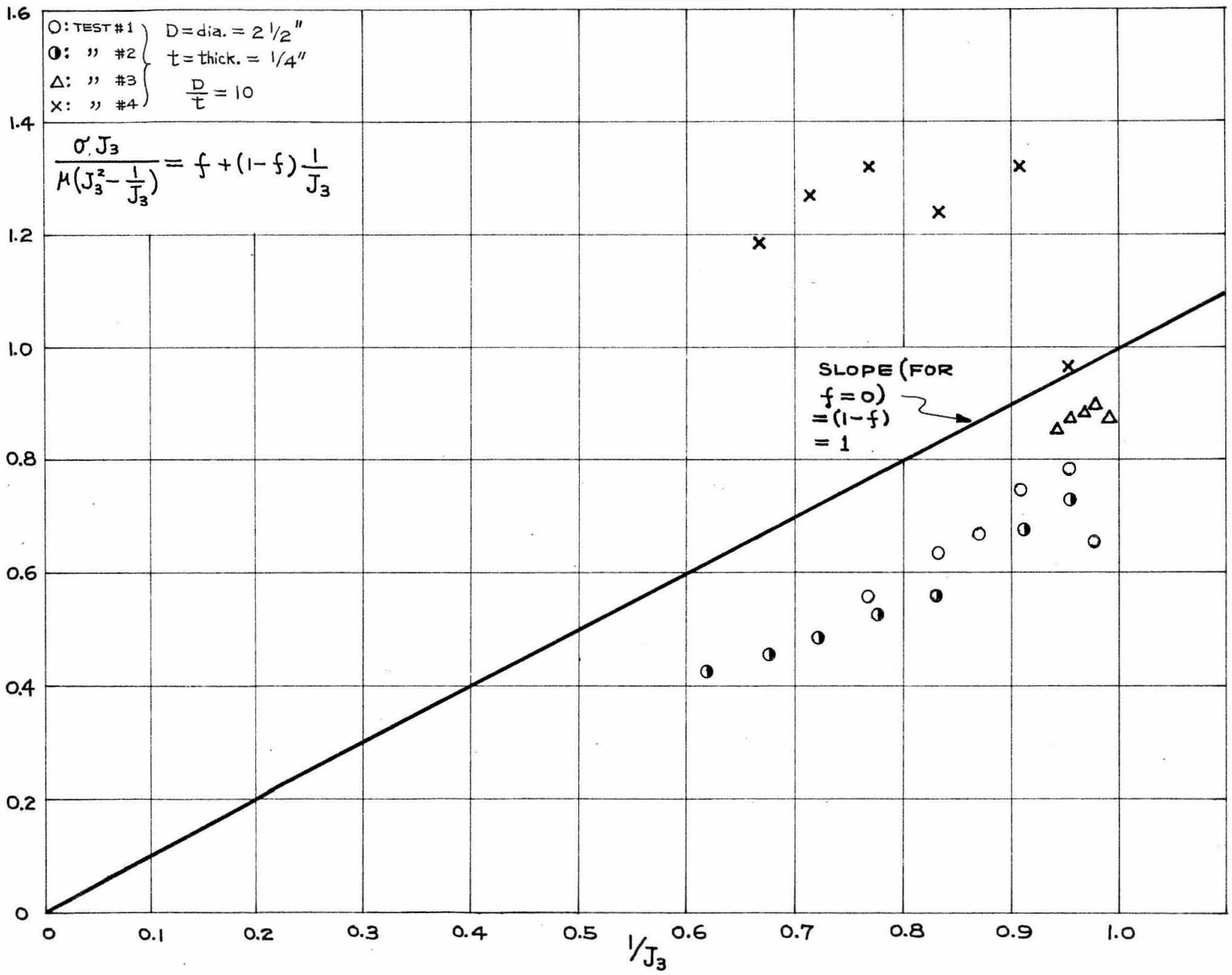

IV. STRESS ANALYSIS CONTINUED

A. Stress Singularities in Wedges

In the last quarterly report the Mellin integral transform was described and it was used to obtain the solution to the problem of an infinite wedge, angle 2α, loaded symmetrically on both of its sides. In the present report we described the extension of this method to the solution of an infinite wedge which is clamped on one side and loaded on the other. The assumed load is a uniform compressive load applied over a finite distance. An extension of this method to any other loading condition is immediately obvious.

1. Formulation

We begin with Equation (IV. 17) of the previous report, this is the biharmonic compatability equation for the transformed stress functions

$$(p+2)^2 p^2 \bar{\phi} + \left[(p+2)^2 + p^2\right] \bar{\phi}_{\theta\theta} + \bar{\phi}_{\theta\theta\theta\theta} = 0 \qquad \text{(IV. 1)}$$

The general solution to the above equation is

$$\bar{\phi} = A \sin p\theta + B \cos p\theta + C \sin (p+2)\theta + D \cos (p+2)\theta \qquad \text{(IV. 2)}$$

The coefficients A, B, C and D are to be evaluated from the boundary conditions. The wedge to be investigated is shown in Figure 1,

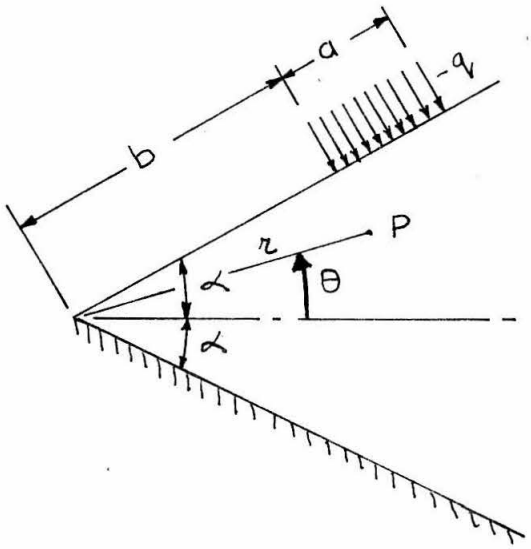

Figure 1.

the side $\Theta = -\alpha$ is assumed to be completely clamped, and on the face $\Theta = \alpha$ a uniform compressive load is applied over a distance 'a' beginning a distance 'b' from the apex. The boundary conditions are therefore,

at $\theta = \alpha$

$$\sigma_\theta = \tau_{r\theta} = 0 \qquad \text{for} \quad 0 < r < b$$

$$\sigma_\theta = -q\,, \quad \tau_{r\theta} = 0 \quad \text{for} \quad b < r < a+b \qquad \text{(IV. 3)}$$

$$\sigma_\theta = \tau_{r\theta} = 0 \qquad \text{for} \quad a+b < r < \infty$$

at $\theta = -\alpha$

$$u = 0\,, \quad v = 0 \qquad \text{(IV. 4)}$$

From equation (IV.20) and (IV.22) of the previous report, the boundary conditions at $\Theta = \alpha$ can be written in the transformed form

$$\bar{\phi} = -q \frac{(a+b)^{p+2} - b^{p+2}}{p(p+1)(p+2)} \qquad \text{(IV.5)}$$

and

$$\bar{\phi}_\theta = 0 \qquad \text{(IV.6)}$$

To transform the boundary conditions at $\Theta = -\alpha$ it is necessary to express the displacements u and v in terms of the stress function ϕ. The necessary relations are given by the strain-stress law.

$$2\mu r^2 u_r = (1-\sigma) r \phi_r + (1-\sigma) \phi_{\theta\theta} - \sigma r^2 \phi_{rr} \qquad \text{(IV.7a)}$$

$$2\mu(r u + r v_\theta) = (1-\sigma) r^2 \phi_{rr} - \sigma r \phi_r - \sigma \phi_{\theta\theta} \qquad \text{(IV.7b)}$$

$$2\mu(r u_\theta + r^2 v_r - r v) = 2\phi_\theta - 2r\phi_{r\theta} \qquad \text{(IV.7c)}$$

Defining the Mellin transforms

$$\bar{u} = \int_0^\infty r u\, r^{p-1}\, dp$$

and

$$\bar{v} = \int_0^\infty r v\, r^{p-1}\, dp$$

the transforms of equations (IV. 7) are

$$2\mu\left[-(p+1)\bar{u}\right] = -(1-\sigma)p\bar{\phi} + (1-\sigma)\bar{\phi}_{\theta\theta} - \sigma(p+1)p\bar{\phi} \qquad \text{(IV. 8a)}$$

$$2\mu\left[\bar{u} + \bar{v}_\theta\right] = \left[(1-\sigma)p(p+1) + \sigma p\right]\bar{\phi} - \sigma\bar{\phi}_{\theta\theta} \qquad \text{(IV. 8b)}$$

$$2\mu\left[\bar{u}_\theta - (p+2)\bar{v}\right] = 2\bar{\phi}_\theta(p+1) \qquad \text{(IV. 8c)}$$

from (IV. 8a)

$$2\mu\bar{u} = \frac{p(1+\sigma p)}{1+p}\bar{\phi} - \frac{1-\sigma}{1+p}\bar{\phi}_{\theta\theta} \qquad \text{(IV. 9)}$$

differentiating (IV. 9) once and substituting into (IV. 8c) for $\bar{u}_\theta$ it follows

$$2\mu\bar{v} = \left[\frac{p(1+\sigma p)}{(p+1)(p+2)} - \frac{2(p+1)}{p+2}\right]\bar{\phi}_\theta - \frac{1-\sigma}{(p+1)(p+2)}\bar{\phi}_{\theta\theta\theta} \qquad \text{(IV. 10)}$$

Therefore the boundary conditions at $\theta = -\alpha$ in the transformed form are

$$p(1+\sigma p)\bar{\phi} - (1-\sigma)\bar{\phi}_{\theta\theta} = 0 \qquad \text{(IV. 11)}$$

and

$$\left[p(1+\sigma p) - 2(p+1)^2\right]\bar{\phi}_\theta - (1-\sigma)\bar{\phi}_{\theta\theta\theta} = 0 \qquad \text{(IV. 12)}$$

By substituting from (IV. 2) into equations (IV. 5), (IV. 6), (IV. 11) and (IV. 12) four algebraic equations in A, B, C and D are obtained.

$$A\sin p\alpha + B\cos p\alpha + C\sin(p+2)\alpha + D\cos(p+2)\alpha = -q\frac{(a+b)^{p+2} - b^{p+2}}{p(p+1)(p+2)} \qquad \text{(IV. 13a)}$$

$$Ap\cos p\alpha - Bp\sin p\alpha + C(p+2)\cos(p+2)\alpha - D(p+2)\sin(p+2)\alpha = 0 \qquad \text{(IV. 13b)}$$

$$Ap\sin p\alpha - Bp\cos p\alpha + C(p+4-4\sigma)\sin(p+2)\alpha - D(p+4-4\sigma)\sin(p+2)\alpha = 0 \qquad \text{(IV. 13c)}$$

$$Ap\cos p\alpha + Bp\sin p\alpha + C(p-2+4\sigma)\cos(p+2)\alpha + D(p-2+4\sigma)\sin(p+2)\alpha = 0 \qquad \text{(IV. 13d)}$$

By putting p = p - 1 the solution to equations (IV. 13) has the form

$$A = -\frac{(p-1+2\sigma)\cos(p+1)\alpha}{(p-1)\cos(p-1)\alpha} C + \frac{(2-2\sigma)\sin(p+1)\alpha}{(p-1)\cos(p-1)\alpha} D \qquad \text{(IV. 14a)}$$

$$B = \frac{(2-2\sigma)\cos(p+1)\alpha}{(p-1)\sin(p-1)\alpha} C - \frac{(p-1+2\sigma)\sin(p+1)\alpha}{(p-1)\sin(p-1)\alpha} D \qquad \text{(IV. 14b)}$$

$$C = -q\frac{(a+b)^{p+1} - b^{p+1}}{P(p+1)}\left[\frac{(p+3-4\sigma)\cos(p+1)\alpha\sin 2(p-1)\alpha - (p-3+4\sigma)\sin(p+1)\alpha\cos 2(p-1)\alpha - (p+1)\sin(p+1)\alpha}{Z(\alpha, p)}\right] \qquad \text{(IV. 14c)}$$

$$D = -q\frac{(a+b)^{p+1} - b^{p+1}}{P(p+1)}\left[\frac{(p+3-4\sigma)\sin(p+1)\alpha\sin 2(p-1)\alpha + (p-3+4\sigma)\cos(p+1)\alpha\cos 2(p-1)\alpha - (p+1)\cos(p+1)\alpha}{Z(\alpha, p)}\right] \qquad \text{(IV. 14d)}$$

where

$$Z(\alpha, p) = -4\left[(3-4\sigma)\sin^2 2p\alpha + p^2\sin^2 2\alpha - 4(1-\sigma)^2\right] \qquad \text{(IV. 15)}$$

The formal solution for the stress function ϕ can now be written in terms of the Mellin inverse integral

$$\phi = \frac{1}{2\pi i}\int_{c-i\infty}^{c+i\infty} \bar{\phi}\, r^{-p+1}\, dp \qquad \text{(IV. 16)}$$

The value of the above integral will depend on the distribution of the poles of $\bar{\phi}$, in the p-plane, and on the path of integration. The final choice of the path of integration has to be based on the physical aspects of the problem. The poles of $\bar{\phi}$ are given by $p = -1$, $p = 0$, $p = 1$, and by the roots of

$$Z(\alpha, p) = 0$$

or

$$(3-4\sigma)\sin^2 2p\alpha + p^2\sin^2 2\alpha - 4(1-\sigma)^2 = 0 \qquad \text{(IV. 17)}$$

It is interesting to note that equation (IV. 17) corresponds to the eigen-equation for the case of a free-clamped sector obtained by Williams.*

---

* Williams, M. L., "Stress Singularities Resulting from Various Boundary Conditions in Angular Corners of Plates in Extension." Journal of Applied Mechanics, vol. 19, 1952.

It is easy to see that the roots of equation (IV. 17) will depend on the angle of the wedge. In general the roots can be calculated in the following way. Equation (IV. 17) is rewritten

$$\sin^2 2p\alpha + (2\alpha p)^2 B - A = 0 \qquad \text{(IV. 18)}$$

where

$$A = \frac{4(1-\sigma)^2}{3-4\sigma}$$

$$B = \frac{1}{3-4\sigma}\left(\frac{\sin 2\alpha}{2\alpha}\right)^2$$

Making the substitution

$$2\alpha p = \beta + i\gamma$$

equation (IV. 18) can be broken up into real and imaginary parts

$$1 - \cos 2\beta \cosh 2\gamma = 2A - 2B(\beta^2 - \gamma^2) \qquad \text{(IV. 19a)}$$

$$\sin 2\beta \sinh 2\gamma = -4B\beta\gamma \qquad \text{(IV. 19b)}$$

From (IV. 19a)

$$\cos^2 2\beta = \frac{\left[1 - 2A + 2B(\beta^2 - \gamma^2)\right]^2}{\cosh^2 2\gamma} \qquad \text{(IV. 20)}$$

and from (IV. 19b)

$$\sin^2 2\beta = \frac{16 B^2 \beta^2 \gamma^2}{\sinh^2 2\gamma} \qquad \text{(IV. 21)}$$

Adding (IV. 20) and (IV. 21) and re-grouping the terms

$$\frac{4B^2}{\cosh^2 2\gamma}\beta^4 + \left[\frac{4B(1-2A-2B\gamma^2)}{\cosh^2 2\gamma} + \frac{16 B^2 \gamma^2}{\sinh^2 2\gamma}\right]\beta^2 + \frac{(1-2A-2B\gamma^2)^2}{\cosh^2 2\gamma} - 1 = 0 \qquad \text{(IV. 22)}$$

Equation (IV. 22) has the form

$$X\beta^4 + Y\beta^2 + Z = 0$$

solving for β

$$\beta = \pm \sqrt{\frac{-Y \pm \sqrt{Y^2 - 4XZ}}{2X}} \qquad \text{(IV. 23)}$$

Substituting from (IV. 23) into (IV. 19b), an equation in γ only is obtained

$$\frac{\sin\left\{\pm 2\sqrt{\frac{-Y \pm \sqrt{Y^2-4XZ}}{2X}}\right\}}{\pm 2\sqrt{\frac{-Y \pm \sqrt{Y^2-4XZ}}{2X}}} = -\frac{2B\gamma}{\sinh 2\gamma} \qquad \text{(IV. 24)}$$

Equation (IV. 24) can be solved very easily by graphical methods. By actual calculation it has been found that only the positive sign, in front of the second square root sign, allows possible solutions of (IV. 24). Once a value of γ has been found the corresponding β can be evaluated from

$$\beta = \pm\sqrt{\frac{-Y + \sqrt{Y^2-4XZ}}{2X}}$$

There are an infinite number of values of γ which will satisfy equation (IV. 24), in general for each value of γ there will be a distinct value of β. It is obvious from the above equations that the roots of (IV. 18) will consist of an infinite number of conjugate pairs symmetrically distributed about the imaginary axis. During the solution of equation (IV. 24) it becomes obvious that β and γ can be expressed in approximate but simple form

$$\beta = n\pi \qquad \text{(IV. 25a)}$$

$$\gamma = \tfrac{1}{2}\ln\{4B(n\pi)^2\} \qquad \text{(IV. 25b)}$$

where $n = 1, 2, 3, \ldots\ldots\ldots$

Equation (IV. 25a) follows from (IV. 24) and (IV. 25b) is obtained by substituting into (IV. 19a) for β. Using the above approximate expressions we have

$$p = \pm \left[\frac{n\pi}{2\alpha} \pm \frac{1}{4\alpha} \ln \left\{ 4B(n\pi)^2 \right\} \right] . \qquad \text{(IV. 26)}$$

Any real solutions to equation (IV. 18) can be obtained from (IV. 19a) by putting $\gamma = 0$, then,

$$\cos 2\beta = 1 - 2A + 2B\beta^2 \qquad \text{(IV. 27)}$$

solutions to (IV. 27) can easily be obtained by numerical methods. It can easily be shown from (IV. 19a) that purely imaginary solution, that is $\beta = 0$, is not possible for any value of the angle α.

For any particular case once the poles of $\bar{\phi}$ have been established it remains to evaluate the line integral in equation (IV. 16). This can be done by changing the line integral to a contour integral and using the residue theory. The contour integral is obtained by closing the line integral by an arc at infinity. It can be shown that the integral along the arc is equal to zero if the following rules are followed. For the region $0 < r < b$ the contour has to be completed to the left of the line integral. For the region $b < r < a + b$ the integral (IV. 16) has to be divided into two parts, one integral containing terms $(a + b)^{p-1}$ and the other b^{p-1}. The line integral containing $(a + b)^{p-1}$ has to be completed to the left and the integral containing b^{p-1} to the right. For the third region $a + b < r < \infty$ the line integral has to be completed to the right. For the special case $b = 0$ the line integral has to be completed to the left or to the right depending whether $r < a$ or $r > a$. We shall now apply this method to two special cases.

2. Wedge Angle $2\alpha = 30^\circ$

It will be assumed that $b = 0$, this will not change the nature of the problem. It shall further be assumed that the wedge is in a condition of plane strain, therefore if the Poisson's ratio for the material is taken as 0.3, then $\sigma = 0.3$.

Under these conditions the real root and the lowest two complex roots of equation (IV.18) have been calculated. These roots, together with the approximate values as calculated from equation (IV.26), are given in Table 1.

Exact		Approximate	
β	γ	β	γ
0.935	0		
2.548	1.38	3.14	1.49
5.834	2.16	6.25	2.20

Figure 1.

It can be noted that the approximation becomes closer as we go down the table.

In Figure 2 the position of the poles of $\bar{\phi}$ are shown. Included in this figure are the poles corresponding to the values in Table 1 plus the three poles on the real axis $p = -1, 0, 1$. All these poles are simple.

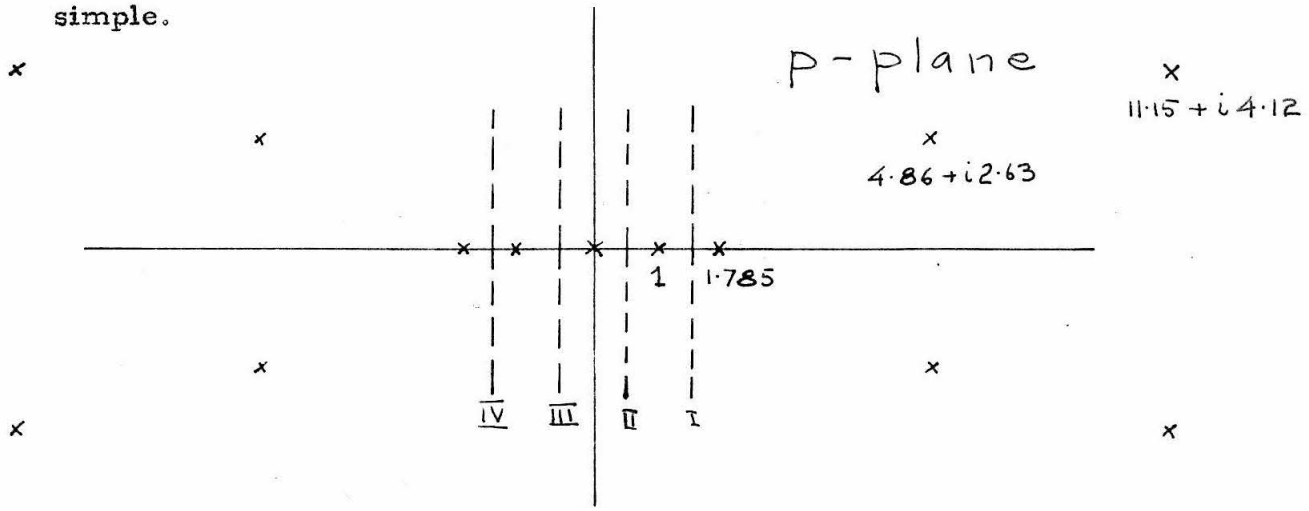

Figure 2.

It remains now to establish the position of the line of integration in equation (IV. 16), for this particular case. Let us first consider the four paths shown in Figure 2. Using path 1 the stress function for the region $r < a$ has the form

$$\phi = -q\frac{a^2}{2} + qar(\sin\alpha\sin\theta + \cos\alpha\cos\theta)$$

$$-q\frac{r^2}{2}\frac{(0.4\sin 2\alpha\sin 2\theta + 0.4\cos 2\alpha\cos 2\theta + \cos 4\alpha)}{0.4 + \cos 4\alpha} \qquad \text{(IV. 28)}$$

+ power series of $\left(\frac{r}{a}\right)$.

The first term in (IV. 28) arises from the pole at $p = 1$, the second from the pole at $p = 0$ and the third from the pole at $p = -1$. The infinite power series is produced by the poles to the left of $p = -1$ and the lowest power of $\frac{r}{a}$ in this series is 0. 785. Since the first term is a constant the path of integration can be moved over $p = 1$ without any physical change. The second term contains $r \sin\theta$ and $r\cos\theta$ and therefore it can be shown that this term does not generate any stresses. It follows that the path of integration can be moved across $p = 0$ without any physical change. Therefore paths I, II, and III are equivalent. If the path IV is used the third term in (IV. 28) drops out. It can be easily shown, however, that in the final solution it is necessary to retain this term in order that the boundary condition at $\theta = \alpha$ may be satisfied. Therefore it follows that path of integration must be to the right of $p = -1$. Let us now consider a path to the right of $p = 1.785$. The residue of the pole at $p = 1.785$ produces a term in the stress function which gives rise to a singularity in the stresses at the apex of the wedge. The order of this singularity is 1. 215. It can easily be shown that stresses with such a singularity are physically unacceptable, for example if the total tangantial load is calculated on any radial line, i. e.,

$$\int_0^\infty \sigma_\theta \, dr$$

the resultant will be an infinite force and physically this is not possible.

Therefore the line of integration has to lie between $p = -1$ and $p = 1.785$. Nothing has been said about the stresses in the region $r > a$, however it can easily be checked that the above line of integration gives physically acceptable stresses in this region also. Since the line of integration, in the inverse transform, has been established it is now possible to obtain the final form of the stress function and therefore the stresses. The stress function so obtained is in the form of an infinite series which arises from the infinite number of poles of ϕ . It can be shown however, just as in the case described in the previous report, that this series converges rapidly especially when $r << a$ or $r >> a$ and therefore for any practical application only first few terms have to be considered.

3. Wedge Angle $2\alpha = 2\pi$

This case corresponds to a crack. For this case equations (IV. 19a) and (IV. 19b) have a simple form

$$\cos 2\beta \cosh 2\gamma = 1-2A \qquad \text{(IV. 29a)}$$

$$\sin 2\beta \sinh 2\gamma = 0 \qquad \text{(IV. 29b)}$$

the solution to these two equations can be very easily obtained, assuming $\sigma = 0.3$,

$$\beta = \pm n \frac{\pi}{2} \qquad \text{(IV. 30a)}$$

$$\gamma = \pm 0.588 \qquad \text{(IV. 30b)}$$

where $n = 1, 3, 5 \ldots$

Therefore the poles of $\bar{\Phi}$ are given by $p = -1$, $p = 0$, $p = 1$ and

$$p = \pm \left(\frac{n}{4} \pm i\, 0.0467 \right)$$

where $n = 1, 3, 5$ etc.

The position of some of these poles is shown in Figure 3.

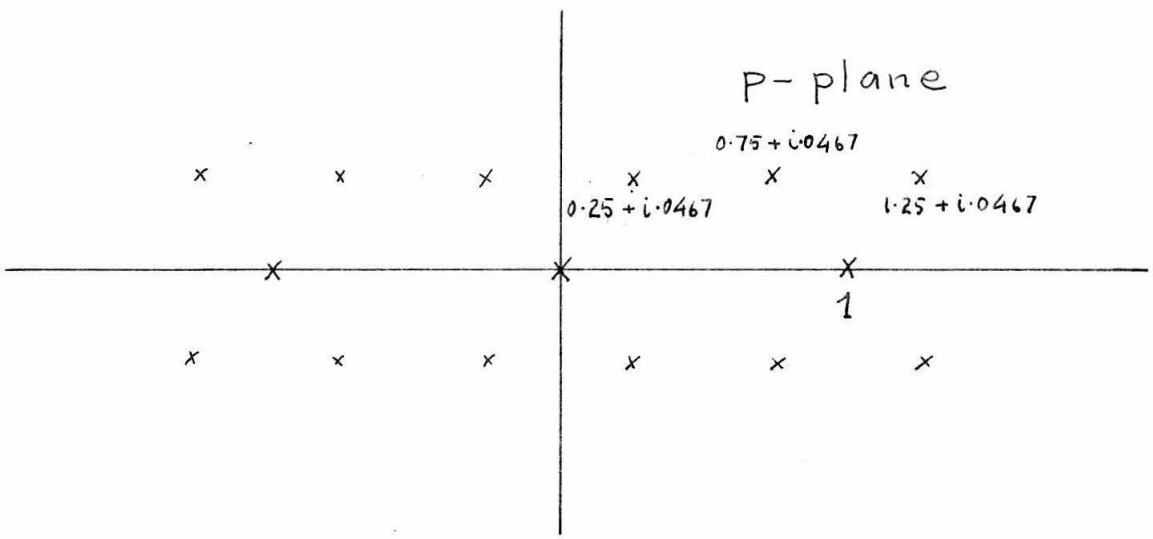

Figure 3.

Using the same arguments as for the case $2\alpha = 30^{\circ}$ it can be established that the path of integration has to lie between $p = -1$ and $p = 0.25$. Introducing a further requirement that the total forces on the wedge at $r = \infty$ have to be finite establishes that the path of integration has to be to the right of $p = -.25$. Therefore the region in which the line integral has to be taken is the strip defined by $p = -.25$ and $p = .25$. It can easily be shown that the path of integration in this region produces a singularity in the stresses at $r = 0$. This singularity is proportional to $r^{0.75}$.

The final solution for the stress function, and therefore the stresses, is again in the form of an infinite series and for any practical application a finite number of terms in these series would have to be used.

4. Closing Remarks

In the previous quarterly report the Mellin Integral Transform was described and was used to find a solution to the problem of an infinite wedge loaded on both of its sides. In the present report the same method has been used to treat a clamped-free wedge which is loaded on the free side. For the purpose of illustration simple loads were considered however an extension to any other more general loading is immediately obvious. The exact solutions obtained are in the form of an infinite series but for practical applications, only a few of the terms in the series have to be considered.

Although, strictly speaking, the method of Mellin Transform can only be applied to infinite wedges nevertheless it can be used to give very good approximate solution for finite wedges. This will be true if the region under interest is a certain distance from the apex which is small compared to the overall dimensions of the wedge.

In order to establish the strip of regularity for the inverse integral it was found necessary to consider many physical aspects of the problem. These aspects were carefully outlined in both reports. It is found that both in the case of the free-free wedge, described in

the previous report, and clamped-free wedge, described in the present report, the factors that affect the choice of the path of integration are similar.

In closing it should be stated that some of the algebraic details, which were presented in the previous report, were omitted from the present one for the sake of clarity. Inclusions of these would produce unnecessary duplication.

B. Stress Singularities in Cylindrical Bodies

1. Introduction

When a cylinder is rigidly clamped on a circular section which is perpendicular to the cylindrical axis, or on the outside cylindrical surface, a circular line of discontinuity is produced. Previous theoretical investigations, see for example references (1) and (2), indicate that the stresses in the neighbourhood of such a discontinuity become very large. However, since the convergence of all the previously obtained solutions is extremely slow in the vicinity of the discontinuity, they are not able to establish definitely whether a stress singularity exists. Therefore, in the present analysis, a method is developed to investigate the presence of such singularities, and if they exist, to establish their strength. This method can also be used in establishing the stress distribution in the vicinity of the discontinuity.

An application of this investigation to the stress analysis in the field of solid propellant rocketry can easily be found. The "poker-chip" test is very widely used to establish the mechanical properties of propellants under tri-axial stress conditions. The specimen in this test corresponds to a short cylinder which is rigidly clamped at both ends and therefore the present analysis can be used to establish the stresses in the vicinity of the lines of discontinuity. In certain case-bonded solid propellant rockets the outside cylindrical surface of the propelland can be considered to be rigorously clamped to the case, under such conditions the

present analysis can again be used to establish the stresses in the vicinity of the discontinuity.

2. The Analysis

The axi-symmetric stress problem of a circular cylinder can be formulated in terms of a stress function $F(r, z)$[3]*, where r and z are the cylindrical coordinates. This stress function is such that it satisfies the compatability conditions and one of the equilibrium equations, in order that the remaining equilibrium equation be satisfied the function F has to be the solution to the following differential equation

$$\nabla^4 F = 0 \tag{IV.31}$$

which, in terms of cylindrical coordinates, has the differential form

$$\left(\frac{\partial}{\partial r^2} + \frac{1}{r}\frac{\partial}{\partial r} + \frac{\partial}{\partial z^2}\right)\left(\frac{\partial^2 F}{\partial r^2} + \frac{1}{r}\frac{\partial F}{\partial r} + \frac{\partial^2 F}{\partial z^2}\right) = 0 \tag{IV.32}$$

The stresses in terms of this stress function have the form

---

* Numbers in the superscripts refer to the reference list.

$$\sigma_r = \frac{\partial}{\partial z}\left(\nu \nabla^2 F - \frac{\partial^2 F}{\partial r^2}\right) \qquad \text{(IV. 33a)}$$

$$\sigma_\theta = \frac{\partial}{\partial z}\left(\nu \nabla^2 F - \frac{1}{r}\frac{\partial F}{\partial r}\right) \qquad \text{(IV. 33b)}$$

$$\sigma_z = \frac{\partial}{\partial z}\left((2-\nu)\nabla^2 F - \frac{\partial^2 F}{\partial z^2}\right) \qquad \text{(IV. 33c)}$$

$$\tau_{rz} = \frac{\partial}{\partial r}\left((1-\nu)\nabla^2 F - \frac{\partial^2 F}{\partial z^2}\right) \qquad \text{(IV. 33d)}$$

By introducing the strain-stress relations it can be shown that the radial displacement u and the axial displacement w are related to F in the following way

$$u = -\frac{(1+\nu)}{E}\frac{\partial^2 F}{\partial r \partial z} \qquad \text{(IV. 34a)}$$

$$w = \frac{(1+\nu)}{E}\left[2(1-\nu)\nabla^2 F - \frac{\partial^2 F}{\partial z^2}\right] \qquad \text{(IV. 34b)}$$

A new coordinate system is now introduced, it is shown in Figure 4.

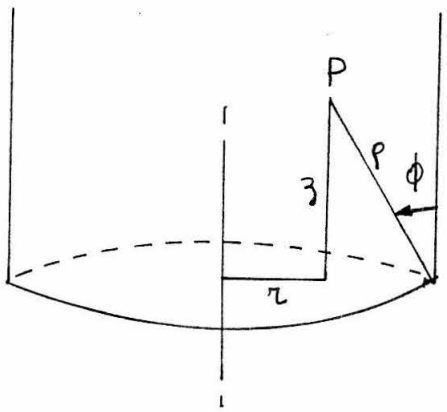

Figure 4.

any point P within the cylinder which has the cylindrical coordinates r and z has now a new set of coordinates ρ and ϕ. The transformation relations between the two coordinate systems is

$$z = \rho\cos\phi \quad , \quad r = 1 - \rho\sin\phi \tag{IV.35}$$

where the radius of the cylinder has been taken as unity, without any loss of generality. It is obvious that the coordinate ρ measures the distance of P from the circumference at one particular axial position on the cylinder, and the angle ϕ the inclination to the vertical of a shortest line joining point P to the same circumference.

The independent variables are now transformed from r, z to ρ , ϕ in equation (IV.32), this gives

$$\left[\frac{\partial^2}{\partial\rho^2} + \frac{1}{\rho^2}\frac{\partial^2}{\partial\phi^2} + \left(\frac{1}{\rho} - \frac{\sin\phi}{1-\rho\sin\phi}\right)\frac{\partial}{\partial\rho} + \left(-\frac{\cos\phi}{\rho(1-\rho\sin\phi)}\right)\frac{\partial}{\partial\phi}\right]$$

$$\times\left[\frac{\partial^2 F}{\partial\rho^2} + \frac{1}{\rho^2}\frac{\partial^2 F}{\partial\phi^2} + \left(\frac{1}{\rho} - \frac{\sin\phi}{1-\rho\sin\phi}\right)\frac{\partial F}{\partial\rho} + \left(-\frac{\cos\phi}{\rho(1-\rho\sin\phi)}\right)\frac{\partial F}{\partial\phi}\right] = 0 \qquad \text{(IV. 36)}$$

let us limit our attention, at present, to the Laplace operator

$$\frac{\partial^2 F}{\partial\rho^2} + \frac{1}{\rho^2}\frac{\partial^2 F}{\partial\phi^2} + \left(\frac{1}{\rho} - \frac{\sin\phi}{1-\rho\sin\phi}\right)\frac{\partial F}{\partial\rho} - \frac{\cos\phi}{\rho(1-\rho\sin\phi)}\frac{\partial F}{\partial\phi} \qquad \text{(IV. 37)}$$

We can now restrict our investigation to the very small region near the circumference, that is where $\rho << 1$, therefore to any desired accuracy (IV. 37) can be approximated by

$$\frac{\partial^2 F}{\partial\rho^2} + \frac{1}{\rho^2}\frac{\partial^2 F}{\partial\phi^2} + \frac{1}{\rho}\frac{\partial F}{\partial\rho} - \frac{\cos\phi}{\rho}\frac{\partial F}{\partial\phi} \qquad \text{(IV. 38)}$$

The first three terms in (IV. 38) are dependent on ρ to the order of $\frac{1}{\rho^2}$ and the last term to $\frac{1}{\rho}$, however at this stage it is not obvious that the last term can be neglected because the derivative $\frac{\partial F}{\partial\phi}$ may be much greater than the other derivatives. We therefore proceed in the following way. Introducing a variable transformation

$$f = \cos\phi \qquad \text{(IV. 39)}$$

(IV. 38) has the form

where the coefficients a, b, c, d and the parameter λ are unknown and have to be determined, for any particular problem, from the boundary conditions.

It is again emphasized here that the solution (IV.44) is only applicable in the immediate neighbourhood of the circumference from where ρ is measured.

3. Case 1 - Cylinder Clamped on Surface Perpendicular to the Axis.

For this case the boundary conditions on the angle ϕ are,

at $\phi = 0$

$$\sigma_r = 0$$

$$\tau_{rz} = 0$$

and in terms of the stress function these have the form, from (IV.33),

$$\frac{\partial}{\partial z}\left(\nu \nabla^2 F - \frac{\partial^2 F}{\partial r^2}\right) = 0 \qquad \text{(IV.45)}$$

$$\frac{\partial}{\partial r}\left((1-\nu)\nabla^2 F - \frac{\partial^2 F}{\partial z^2}\right) = 0 \qquad \text{(IV.46)}$$

at $\phi = \frac{\pi}{2}$

$$u = 0, \quad \text{and} \quad w = 0$$

or, from (IV.34),

$$\frac{\partial^2 F}{\partial r \partial z} = 0 \qquad \text{(IV.47)}$$

$$2(1-\nu)\nabla^2 F - \frac{\partial^2 F}{\partial z^2} = 0 \qquad \text{(IV.48)}$$

After changing the independent variables in equations (IV.45) to (IV.48) to ρ and ϕ the solution (IV.44) is substituted in to these equations. The detailed algebraic steps are omitted from this report because of their length. After the substitution the following four algebraic equations are obtained

$$b\left[\lambda^2+\lambda(3-4\nu)\right] + d\left[\lambda^2-\lambda\right] = 0 \qquad \text{(IV.49)}$$

$$a\left[\lambda^3-\lambda\right] + c(\lambda-1)\left[\lambda^2+\lambda(-5+4\nu)\right] = 0 \qquad \text{(IV.50)}$$

$$-a(\lambda+1)\sin\lambda\tfrac{\pi}{2} - b(\lambda+1)\cos\lambda\tfrac{\pi}{2} + c(\lambda-1)\sin\lambda\tfrac{\pi}{2} + d(\lambda-1)\cos\lambda\tfrac{\pi}{2} = 0 \qquad \text{(IV.51)}$$

$$a(\lambda^2+\lambda)\cos\lambda\tfrac{\pi}{2} - b(\lambda^2+\lambda)\sin\lambda\tfrac{\pi}{2} - c\left[\lambda^2+\lambda(5-8\nu)\right]\cos\lambda\tfrac{\pi}{2} + d\left[\lambda^2+\lambda(5-8\nu)\right]\sin\lambda\tfrac{\pi}{2} = 0 \qquad \text{(IV.52)}$$

In order that a non-trivial solution be possible, the determinant of the coefficients in the above four algebraic equations has to vanish. This gives

$$\lambda^3+\lambda^2(1-4\nu)+\lambda(-4+4\nu+4\nu^2)-24+82\nu-92\nu^2+32\nu^3 + \left[\lambda(2-4\nu)+24-78\nu+88\nu^2-32\nu^3\right]\cos^2\lambda\tfrac{\pi}{2} = 0 \qquad \text{(IV.53)}$$

The characteristic equation (IV. 53) can possibly have real and complex solutions for λ . In order that the displacements, at $\rho = 0$, be bounded the real part of λ has to be greater than unity, as can be seen from equation (IV.33). Furthermore the stress singularities are produced only by the values of λ whose real part lies between 1 and 2, this can be seen from equation (IV.33). Therefore our interest centers on the solution of (IV.53) in this region. It has been assumed that a real solution for λ exists and (IV.53) has been solved for $\nu = 0.3$ and $\nu = 0.45$, the solutions are $\lambda = 1.67$ and $\lambda = 1.63$ respectivly.

Therefore the corr esponding stress variation, in the vicinity of $\rho = 0$, is $\sigma \sim \frac{1}{r^{.33}}$ and $\sigma \sim \frac{1}{r^{.37}}$ for the two different values of the Poisson's ratio. The possibility of complex solution of (IV.53), which may give stronger singularities, has not yet been investigated since much time is required for such a solution, which has to be obtained numerically.

If the singularity for $\nu = 0.3$ is compared with the one for a clamped-free 90° angle wedge under plane stress, analyzed in reference (4), it is seen that in the case of a cylinder, clamped as assumed, the stress singularity is stronger, since for the wedge we have the stress proportional to $\frac{1}{r^{.25}}$. We may also make a directed guess that since in the case of the wedge the stress is of non-oscillating type, that is the singularity comes from the real solution of the characteristic equation, the same behavior can be expected in the case of the cylinder. However this should be checked out by investigating possible complex solution.

4. Case II - Cylinder Clamped on Outside Cylindrical Surface

For this case the boundary conditions are

at $\phi = 0$

$$u = 0, \qquad w = 0$$

or

$$\frac{\partial^2 F}{\partial r \partial z} = 0 \qquad \text{(IV. 54)}$$

$$2(1-\nu)\nabla^2 F - \frac{\partial^2 F}{\partial z^2} = 0 \qquad \text{(IV. 55)}$$

at $\phi = \frac{\pi}{2}$

$$\sigma_z = 0 \quad , \quad \tau_{rz} = 0$$

or

$$\frac{\partial}{\partial z}\left[(2-\nu)\nabla^2 F - \frac{\partial^2 F}{\partial z^2}\right] = 0 \qquad \text{(IV. 56)}$$

$$\frac{\partial}{\partial r}\left[(1-\nu)\nabla^2 F - \frac{\partial^2 F}{\partial z^2}\right] = 0 \qquad \text{(IV. 57)}$$

We proceed as in the Case I and substitute from (IV. 44) into equations (IV. 54) to (IV. 57), the resulting algebraic equations are:

$$a(\lambda+1) + c(\lambda-1) = 0 \qquad \text{(IV. 58)}$$

$$b(-\lambda^2-\lambda) + d\left[-\lambda^2 + \lambda(7-8\nu)\right] = 0 \qquad \text{(IV.59)}$$

$$a(\lambda^2-1)\sin\lambda\tfrac{\pi}{2} + b(\lambda^2-1)\cos\lambda\tfrac{\pi}{2} - c\left[\lambda^2+\lambda(2-4\nu)-3+4\nu\right]\sin\lambda\tfrac{\pi}{2} - d\left[\lambda^2+\lambda(2-4\nu)-3+4\nu\right]\cos\lambda\tfrac{\pi}{2} = 0 \qquad \text{(IV.60)}$$

$$-a(\lambda^2-1)\cos\lambda\tfrac{\pi}{2} + b(\lambda^2-1)\sin\lambda\tfrac{\pi}{2} + c\left[\lambda^2-\lambda 4\nu-1+4\nu\right]\cos\lambda\tfrac{\pi}{2} - d\left[\lambda^2-\lambda 4\nu-1+4\nu\right]\sin\lambda\tfrac{\pi}{2} = 0 \qquad \text{(IV.61)}$$

Again imposing the condition that the determinant of the coefficients has to vanish, the following characteristic equation is obtained:

$$\left[\lambda^3+\lambda^2(-3)+\lambda(-1+8\nu-4\nu^2)+3-8\nu+4\nu^2\right] + \left[\lambda(3-4\nu)-3+8\nu\right]\cos^2\lambda\tfrac{\pi}{2} = 0 \qquad \text{(IV.62)}$$

The real solutions to (IV.62) for ν = 0.3 and 0.45 are λ = 1.96 and 1.24 respectively. These give a stress variation in the vicinity of ρ = 0, as $\sigma \sim \frac{1}{r^{.04}}$ and $\sigma \sim \frac{1}{r^{.76}}$ respectively. As in the previous case the possible complex solutions to (IV.62)

whose real part may lay between 1 and 2 have not yet been investigated, this again will involve much numerical calculations.

5. Conclusions

A method has been developed which enables the investigation of the existance, and strength of stress singularities in cylindrical bodies. The method has been applied to two particular cases. For these two cases the analysis shows that singularities exist for the values of Poisson's ratio chosen. However, whether these are the only singularities in each case can only be answered after much more numerical calculations, which perhaps could be programmed on a digital computer.

REFERENCES

1. Pickett, G., "Application of the Fourier Method to the Solution of Certain Boundary Problems in the Theory of Elasticity." Journal of Applied Mechanics, September 1944, p. A176.

2. Messner, A., "Propellant Grain Stress Analysis." Aerojet-General Corp. (Unpublished)

3. Love, A. E. H., "The Mathematical Theory of Elasticity." Dover Publishing Co., New York, N. Y., 4th edition, 1927.

4. Williams, M. L., "Stress Singularities Resulting from Various Boundary Conditions in Angular Corners of Plates in Extensions." Journal of Applied Mechanics, December 1952, p. 526.